

3-D Analysis of Terahertz Frequency Multiplier Excited Due to Interaction of Convection Electron Beam and Surface Waves (Smith-Purcell Effect)

Alireza Tavousi¹, Ali Rostami^{1,2}, Ghassem Rostami² and Mahboubeh Dolatyari²

¹Photonic and Nanocrystal Research Lab. (PNRL), Faculty of Electrical and Computer Engineering,
University of Tabriz, Tabriz 5166614761, Iran

²OIC Research Group, School of Engineering-Emerging Technologies, University of Tabriz, Tabriz 5166614761, Iran

Keywords: Convection Electron Beam, Terahertz Wave Generation, Smith-Purcell Effect, Surface Wave, Frequency Multiplier.

Abstract: In this paper, we present a three dimensional numerical study on a terahertz frequency multiplier. The process of frequency multiplication is proposed via study of spontaneous Smith-Purcell (SP) radiation. Through introducing a single electron bunch perturbation which is passing over above a metallic grating, and due to interaction of electron bunch with surface wave, the evanescent wave radiates from the ends of the grating and the SP radiation is generated in the span of 0.466~1.1 THz. We found that the maximum of SP radiation amplitude is distributed around 90° with the centre frequency of ~0.65 THz. Simulations on the generation of SP radiation at THz frequencies have been performed with the help of the 3D particle-in-cell (PIC) finite integral method and results agree very well with analytic ones.

1 INTRODUCTION

The ‘terahertz’ term has been applied in diverse electromagnetic spectra such as for frequency coverage of point contact diode detectors (Kerecman, 1973), frequency of a Michelson interferometer (Fleming, 1974), frequencies below the far infrared, the resonant frequency of a water laser, and now terahertz is applied to sub-millimetre wavelengths span between 100 and 1000 μm (0.3 THz to 3 THz) (Siegel, 2002). Until recently there were no appropriate sources and detectors for THz and thus this portion of the EM spectrum has been used just about. Among the most advanced terahertz applications which the scientific research is concerned about, we bring up the followings: medical imaging, security, communications, industrial applications, chemistry and biochemistry measurements, molecular recognition and protein folding, and sub-millimetre astronomy (Rostami *et al.*, 2010).

Smith-Purcell (SP) radiation (Smith & Purcell, 1953) which works based on excitation of “surface Eigen wave” (Bratman *et al.*, 2009; Cao *et al.*, 2014) in metallic gratings, is one of the most interesting methods for generating sub-millimetre waves

especially in THz domain (Bratman *et al.*, 1979; Bratman *et al.*, 2007; Gover & Sprangle, 1981; Liu & Xu, 2014; Mizuno *et al.*, 1973; Price *et al.*, 1991; Rusin & Bogomolov, 1966; Schächter & Ron, 1988). At the frequency harmonics of the surface wave, electron bunches arise and produce spontaneous Smith-Purcell radiation. Due to spontaneous nature of SP radiation as discussed in the most of theoretical works (Andrews & Brau, 2004) and in experiment (Urata *et al.*, 1998) the radiated power is low. But by using an additional cavity, higher power and better selectivity can be obtained (Bratman *et al.*, 2007). This mechanism which is conceptually shown in Figure 1 is frequently studied for electron-beam driven frequency multiplication and undoubtedly it is a promising candidate for producing radiation in the terahertz domain (Andrews & Brau, 2004; Bratman *et al.*, 2009; Li *et al.*, 2006; Shin *et al.*, 2007).

The grating is assumed to be a perfect conductor and unlike the experiment (Urata *et al.*, 1998) with pencil-like electron beams, in the proposed design a sheet electron beam is used which through enhancing the interaction of electron beam and surface wave, increases the operating current and output power. It is known that single-mode

operation of the surface wave in the case of a fairly narrow beam is possible (Li *et al.*, 2007). However when the beam width becomes much larger than the wavelength of the surface mode, different transverse parts of the beam would be able to excite different transverse surface modes which their frequencies and phases are slightly different (Bratman *et al.*, 2009). This is already mentioned for SP backward wave oscillators (BWOs) that they will not operate with an infinitely wide grating because the optical beam diffuse (Li *et al.*, 2007).

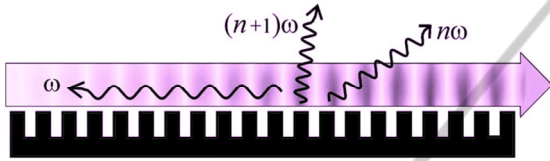


Figure 1: Scheme of an electron-beam driven THz range frequency multiplier which is self-excited due to surface waves of open grating (Bratman *et al.*, 2009).

In this paper, we perform a three-dimensional finite integral based particle-in-cell simulation for the evaluating the incoherent spontaneous SP radiation using CST studio suite, a code which simulates the situations in which the space charge and electromagnetic fields are concurrently interacting.

2 SIMULATION MODEL

Here in this paper, we consider a metallic grating slab having a period L and thus a wave number of $K = 2\pi/L$ (the length of the grating is set differently for each particular simulation case). Generally, an evanescent wave can travel above the surface of such grating in the direction in which the slab is periodic (perpendicular to the grooves). The phase velocity is $v_\phi = \omega/k = c\beta_\phi$, and the group velocity is $v_g = d\omega/dk = \beta_g c$ where c is the speed of light, ω is the frequency of the traveling evanescent wave and k is the wave number. It is known that (Andrews *et al.*, 2006) the dispersion relation is periodic in k space and for each Brillion zone the dispersion curve is symmetric about $k/K = 0.5$ (π -type surface mode). Depending on the position of the synchronous point which may be located on the right-hand or left-hand side of the Bragg point $k/K=0.5$ (for which the group velocity vanishes), the operating characteristics of the device changes fundamentally. For $k/K > 0.5$, the group velocity is negative and for $k/K < 0.5$ the group velocity is positive. Here we are interested in the former case in which the operating point lies in

the negative group velocity regions. If we assume that there is no gain or losses in the grating due to an electron beam then we may use Floquet's theorem in order of solving Maxwell equations on top of the grating and the dispersion relation $D_\theta(\omega, k) = 0$ is obtained for the evanescent waves.

With respect to the operating point, our Smith-Purcell based THz source is a backward wave oscillator in which, if a certain beam current threshold known as start current is reached, the optical intensity grows to saturation even if no feedback mirrors are employed. In this device, the moving electron beam must interact significantly with the fundamental surface mode which is confined very close to the grating. To describe the interaction between the surface mode and the moving electron beam, we need to numerically solve the coupled Maxwell-Lorentz equations. For this purpose, we used the CST studio suite software which solves these coupled equations via finite integral method. The radiation wavelength λ observed at the angle θ measured from the direction of moving electron beam is given by:

$$\frac{\lambda}{L} = \frac{1}{|n|} \left(\frac{1}{\beta_\phi} - \cos\theta \right), \quad (1)$$

where n is the diffraction order. In order to compare our 3-D simulation results with experiment results and 2-D simulations, we chose to use grating parameters of Urata *et al.* (Urata *et al.*, 1998) summarized in Table 1. Since we have performed our simulations in a 3-D scheme, a width of $800 \mu\text{m}$ is used for grating. The grating length is arranged to be 20, 40, 60, 80, and 100 periods. The main simulations are performed using a grating with length $N_g=100$ periods and then the results are extended and compared with grating lengths of $N_g=20, 40, 60,$ and 80 periods.

Table 1: Grating profile used in the experiments of Urata *et al.* (Urata *et al.*, 1998).

Grating period	173 μm
Groove width	62 μm
Groove depth	100 μm

2 SIMULATION RESULTS

The dispersion diagram of the first three modes of a grating with parameters from Table 1 is shown in Figure 2. The 40 Kev beam line intersect with the first mode in negative group velocity region i.e. $k/K > 0.5$, thus the synchronous point frequency

would be calculated as 0.466 THz. For a device operating in positive group velocities, higher beam energies is required. For example in this figure we have shown the 250 Kev beam line which is intersecting the evanescent mode in $k/K < 0.5$ region.

To study the incoherent (spontaneous) SP radiation, first we let the length of the grating to be $N_g=100L$ and then we perform the simulation with a single electron bunch which last for 0.1 ps length and carry a charge equal to $q=0.048$ pC. Since this bunch is short enough compared to the longest radiation wavelength, we can assume that the radiation is coherent. Our focus is on the first order SP radiation ($|n|=1$). As shown in Figure 3a-f, by recording the temporal behaviour of the radiated signal which we have detected them at different detection points of $\theta=70^\circ, 90^\circ, 125^\circ, 135^\circ, 150^\circ$, and 170° (and 5.5 mm distance from the centre of the grating) and taking fast Fourier transform, we find out that two clear radiation peaks exists in the spectrum. Figure 4a shows that the one which peaked at 525 GHz is the SP radiation, while the other peak at 466 GHz is the evanescent wave (for ease of visualization, only FFT of Figure 3c at $\theta=135^\circ$ is shown in Figure 4a).

Figure 4b compares the analytic expression for wavelength of SP radiation with the centre frequencies recorded by sweeping θ with 6° step for all detection angles between $0^\circ < \theta < 180^\circ$. From this figure we find out that indeed the longest radiation wavelength (lowest radiation frequency) is equal to the wavelength of the evanescent wave. The results

obtained from CST are in good agreement with those obtained via equation (1). Recording the FFT amplitude for all swept angles (Figure 5), we find out that unlike the evanescent wave frequency which is angle independent, both SP radiation centre frequency and amplitude are changing with detection angle. As shown in this figure the maximum SP amplitude occurs in angle $\theta=90^\circ$. The short come of this equation is that it says nothing about the SP radiation amplitude.

Given the detection angle, period, diffraction order, and the phase velocity of the electron beam to the analytic equation (1), one can predict the

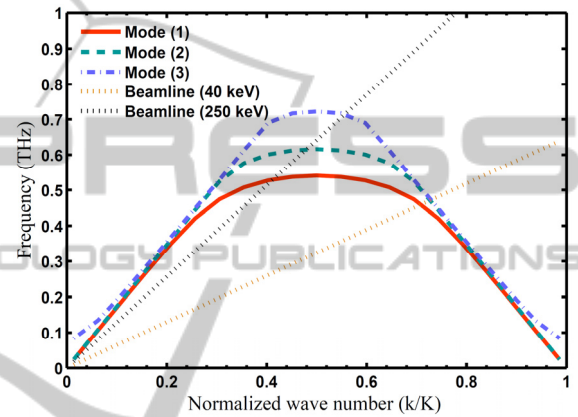


Figure 2: Dispersion diagrams of the first three surface modes of the metallic grating with parameters given in Table 1. The 40 Kev and 250 Kev beam lines intersect with the fundamental mode in $k/K < 0.5$ and $k/K > 0.5$ regions respectively.

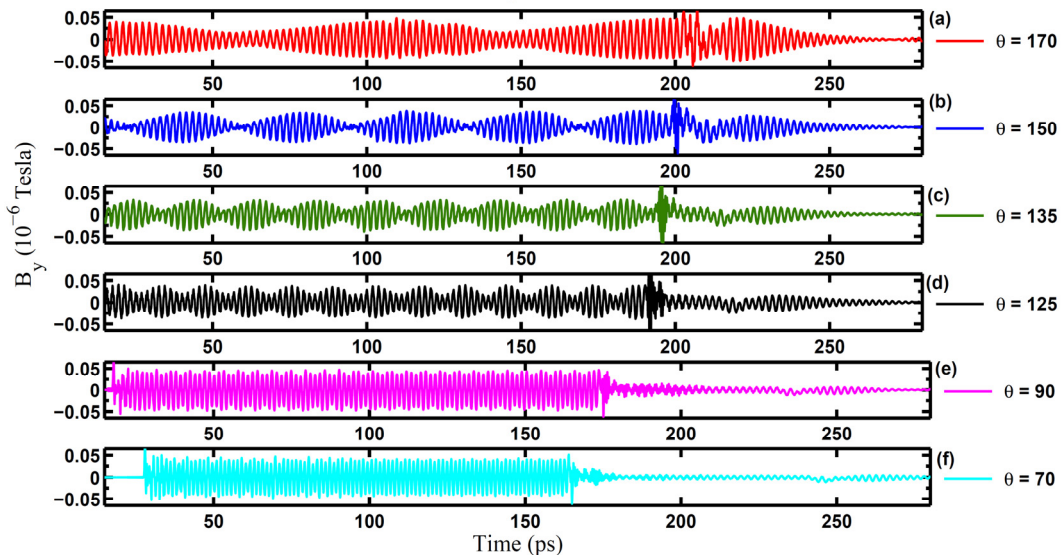


Figure 3: The temporal behaviour of the radiated signal detected at the angle $\theta=135^\circ$ and 5.5 mm distance from the centre of the grating for $N_g=100L$.

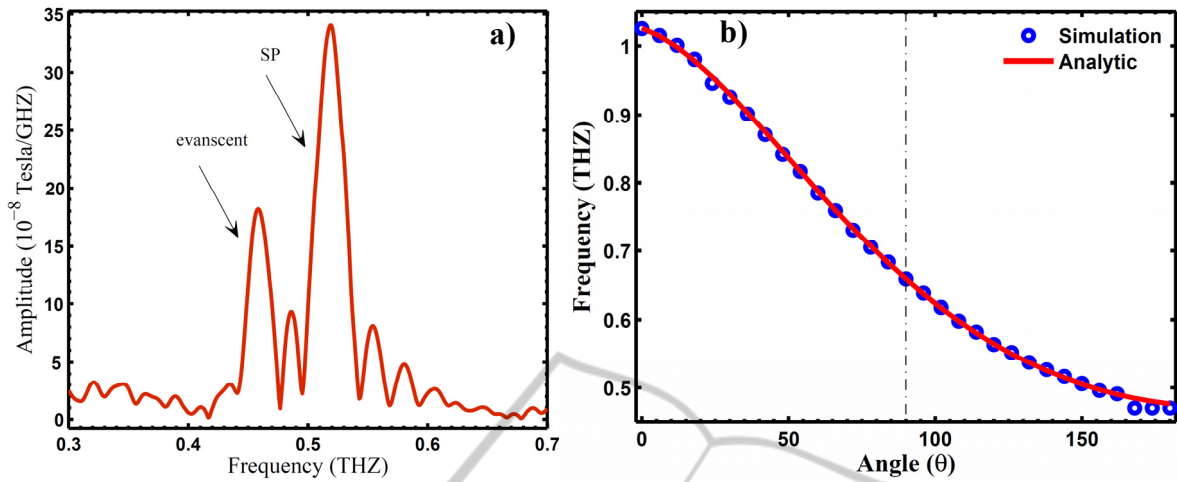


Figure 4: (a) FFT taken from temporal behaviour of the radiated signal detected at the point $\theta=135^\circ$ for $N_g=100L$. (b) Comparison of analytic expression for wavelength of SP radiation with the center of SP frequencies swept from $\theta=0^\circ$ to $\theta=180^\circ$.

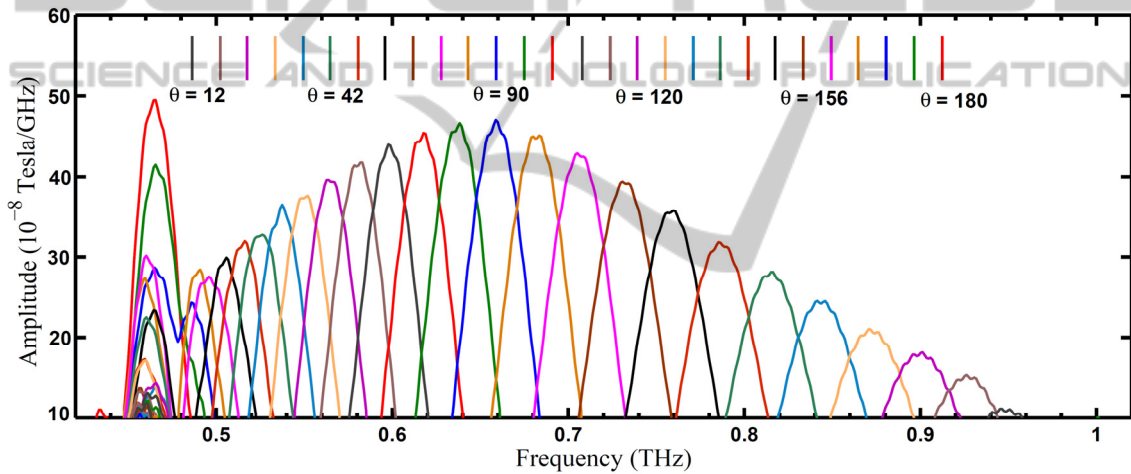


Figure 5: FFT taken from temporal behaviour of the radiated signal detected at the different points varying from $12^\circ < \theta < 180^\circ$ with step of $\Delta\theta = 6^\circ$ for $N_g=100L$.

wavelength in which the SP radiation occurs. Figure 6 shows the normalized far field polar plot for the H-field at different θ angles. These plots show that the main radiation lobe of each specific frequency is located in the angle which was predicted by equation (1). In the 0.466 THz, our result show that radiation occur near 180° , and as we know from previous, this frequency belongs to the evanescent wave so radiates from the upper grating end (near gun). The 0.55 THz, 0.65 THz, and 0.85 THz cases are also radiating at 120° , 90° , and 40° , respectively.

Figure 7a, and Figure 7b both show the FFT amplitudes of time signals for different grating lengths. In Figure 7a, we swept the detection angle from 0° to 180° and recorded the maximum of FFT amplitude for gratings with $N_g=20, 40, 60, 80$, and

$100L$. We can see that, as the length of grating increase from 20 to 100 periods, the amplitude grows nonlinearly. Given this, we are able to calculate the growth-rate of the produced signal. In Figure 7b, focusing only on one detection angle in which the radiation is maximum (i.e. $\theta=90^\circ$), we find out that by increasing the grating length, not only the FFT amplitude increases but the spectral resolution of the signal increases too.

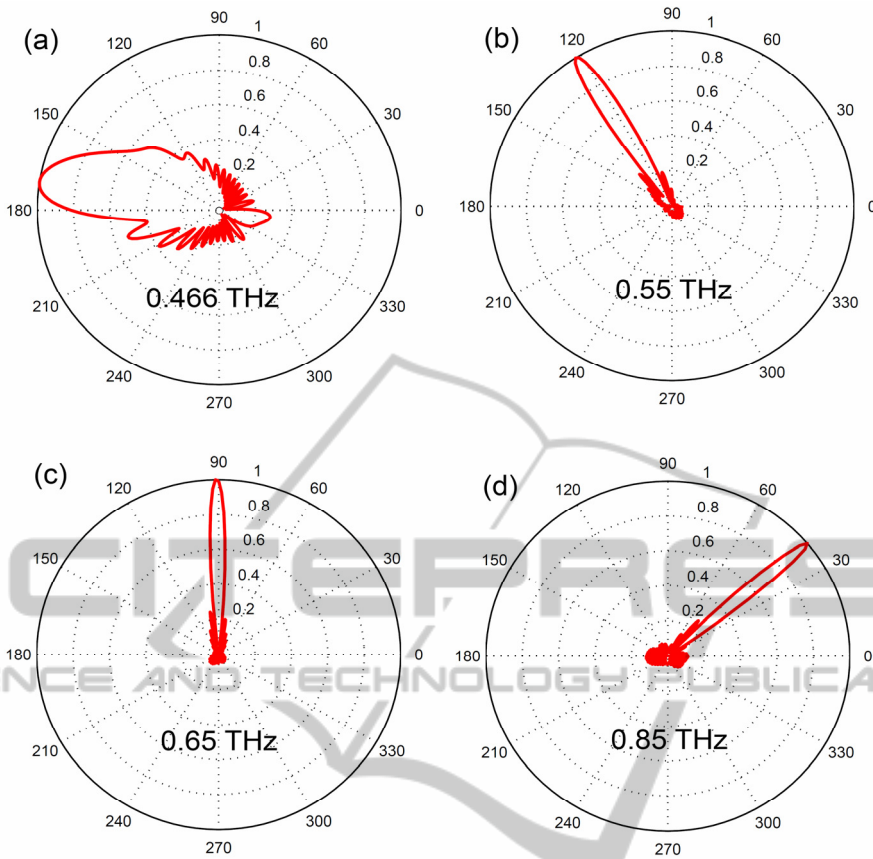


Figure 6: Far field polar plots for H-field at different frequencies of a) 0.466 THz, b) 0.55 THz, c) 0.65 THz, and d) 0.85 THz. The plots are normalized.

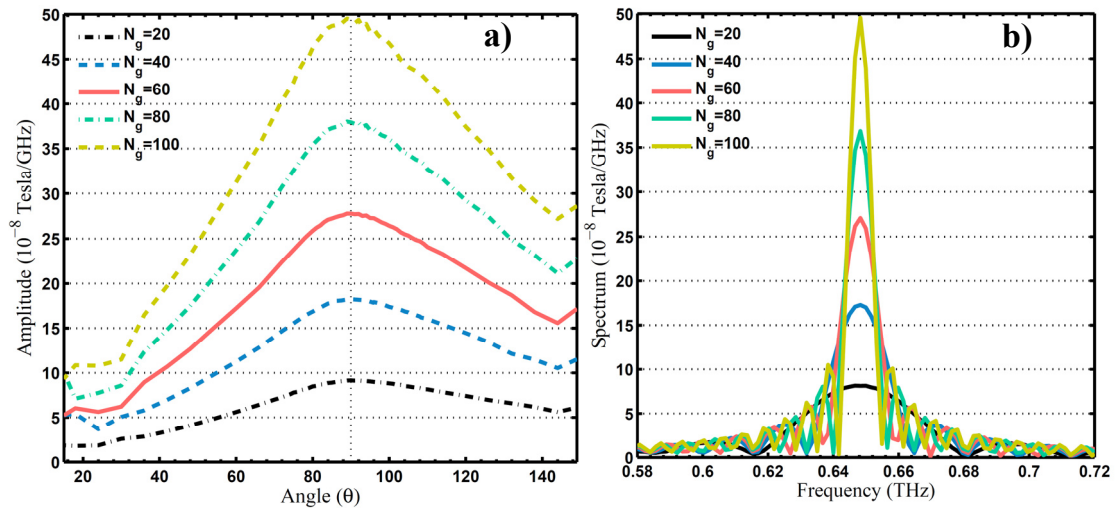


Figure 7: (a) The max FFT amplitude of time signals versus detection angel for different grating widths of $N_g=20L$, $40L$, $60L$, $80L$, and $100L$ (b) The max FFT amplitude of time signals versus detection angel of $\theta=90^\circ$ for different grating widths of $N_g=20L$, $40L$, $60L$, $80L$, and $100L$.

3 CONCLUSIONS

In this paper, we presented a three dimensional numerical study on a terahertz frequency multiplier. This SP based frequency multiplier can provide terahertz radiation with a comparatively high level of output power. The process for frequency multiplication was proposed by studying the spontaneous SP radiation. This non-relativistic device neither requires a high operating voltage nor a high external magnetic field. It can fill up the need for convenient compact THz radiation source for diverse range of applications such as spectroscopy and diagnostics of different media. Simulations on the generation of SP radiation at THz frequencies have been performed with the help of the 3D particle-in-cell (PIC) finite integral method and results agree very well with analytic ones.

ACKNOWLEDGEMENTS

The authors would like to thank University of Tabriz.

REFERENCES

Andrews, H. L., Boulware, C., Brau, C., Donohue, J., Gardelle, J., & Jarvis, J. (2006). Effect of reflections and losses in Smith-Purcell free-electron lasers. *New Journal of Physics*, 8(11), 289.

Andrews, H. L., & Brau, C. A. (2004). Gain of a Smith-Purcell free-electron laser. *Physical Review Special Topics - Accelerators and Beams*, 7(7), 070701.

Bratman, V. L., Fedotov, A. E., Makhalov, P. B., & Rusin, F. S. (2009). Smith-Purcell frequency multiplier with synchronization of radiation from a wide electron beam. *Applied Physics Letters*, 94(6), 061501.

Bratman, V. L., Ginzburg, N., & Petelin, M. (1979). Common properties of free electron lasers. *Optics Communications*, 30(3), 409-412.

Bratman, V. L., Makhalov, P., Fedotov, A., & Khaimovich, I. (2007). Excitation of orotron oscillations at the doubled frequency of a surface wave. *Radiophysics and Quantum Electronics*, 50(10-11), 780-785.

Cao, M., Liu, W., Wang, Y., & Li, K. (2014). Three-dimensional theory of Smith-Purcell free-electron laser with dielectric loaded grating. *Journal of Applied Physics*, 116(10), 103104.

Fleming, J. (1974). High-resolution submillimeter-wave Fourier-transform spectrometry of gases. *IEEE Transactions on Microwave Theory Techniques*, 22, 1023-1025.

Gover, A., & Sprangle, P. (1981). A unified theory of magnetic bremsstrahlung, electrostatic bremsstrahlung, Compton-Raman scattering, and Cerenkov-Smith-Purcell free-electron lasers. *Quantum Electronics, IEEE Journal of*, 17(7), 1196-1215.

Kerecman, A. J. (1973). *The Tungsten-P Type Silicon Point Contact Diode*. Paper presented at the Microwave Symposium, 1973 IEEE G-MTT International.

Li, D., Imasaki, K., Gao, X., Yang, Z., & Park, G.-S. (2007). Reduce the start current of Smith-Purcell backward wave oscillator by sidewall grating. *Applied Physics Letters*, 91(22), 221506.

Li, D., Imasaki, K., Yang, Z., & Park, G.-S. (2006). Three-dimensional simulation of super-radiant Smith-Purcell radiation. *Applied physics letters*, 88(20), 201501.

Liu, W., & Xu, Z. (2014). Simulations of table-top watt-class 1 THz radiation sources with two-section periodic structure. *Journal of Applied Physics*, 115(1), 014503.

Mizuno, K., Ono, S., & Shibata, Y. (1973). Two different mode interactions in an electron tube with a Fabry-Perot resonator-The Ledatron. *Electron Devices, IEEE Transactions on*, 20(8), 749-752.

Price, E., Walsh, J., & Kimmitt, M. (1991). Short submillimeter operation of the Planar Orotion. *Nuclear Instruments and Methods in Physics Research Section A: Accelerators, Spectrometers, Detectors and Associated Equipment*, 304(1), 133-136.

Rostami, A., Rasooli, H., & Baghban, H. (2010). *Terahertz technology: fundamentals and applications* (Vol. 77): Springer.

Rusin, F., & Bogomolov, G. (1966). Generation of electromagnetic oscillations in an open resonator. *JETP Letters*, 4, 160-162.

Schächter, L., & Ron, A. (1988). Exponential gain in a Smith-Purcell amplifier. *Applied physics letters*, 53(10), 828-830.

Shin, Y.-M., So, J.-K., Jang, K.-H., Won, J.-H., Srivastava, A., & Park, G.-S. (2007). Superradiant terahertz Smith-Purcell radiation from surface plasmon excited by counterstreaming electron beams. *Applied Physics Letters*, 90(3), 031502.

Siegel, P. H. (2002). Terahertz technology. *IEEE Transactions on microwave theory and techniques*, 50(3), 910-928.

Smith, S. J., & Purcell, E. M. (1953). Visible Light from Localized Surface Charges Moving across a Grating. *Physical Review*, 92(4), 1069-1069.

Urata, J., Goldstein, M., Kimmitt, M. F., Naumov, A., Platt, C., & Walsh, J. E. (1998). Superradiant Smith-Purcell Emission. *Physical Review Letters*, 80(3), 516-519.